Oil Shale, 2024, Vol. 41, No. 3, pp. 208–235
doi: https://doi.org/10.3176/oil.2024.3.04
ISSN 0208-189X

Co-pyrolysis of biomass woodchips with Ca-rich oil shale fuel in a continuous feed reactor

Alejandro Lyons Ceron*, Tõnu Pihu, Alar Konist

Department of Energy Technology, Tallinn University of Technology, Ehitajate tee 5, 19086 Tallinn, Estonia

Received 13 March 2024, accepted 12 July 2024, available online 5 August 2024

Abstract. *A co-pyrolysis of woodchips and oil shale was conducted in a continuous reactor at 520 °C in a CO_2 atmosphere. Experimental product yields were derived and an analysis of the liquid products was conducted, using gas chromatography, infrared spectroscopy, and physicochemical analysis. A maximum yield of liquids and gases was obtained as the share of biomass increased (43.9 and 35.1 wt%, respectively). Product characterization confirmed additive behavior in co-pyrolysis. The liquid products from co-pyrolysis blends exhibited fewer oxygenated compounds, derived from biomass, and fewer aromatic compounds, derived from oil shale. Co-pyrolysis liquids contained abundant aliphatic hydrocarbons (C_6 to C_{11}).*

Keywords: *thermochemical conversion, co-pyrolysis, continuous feed reactor, oil shale, woodchips.*

1. Introduction

Utilizing alternative and clean energy solutions offers the potential to mitigate the environmental impact of using conventional fossil fuels for energy production by decreasing pollutant gas emissions and reducing reliance on non-renewable resources [1]. One approach to a carbon-neutral transition is the co-conversion of renewable resources, such as biomass, and fossil resources, such as oil shale (OS). Both fuels are utilized in thermochemical conversion processes to produce solid, liquid, and gaseous products with valuable applications in the energy sector and the chemical industry [2].

Biomass has been widely used and studied as a resource to produce energy and valuable products. It stands out as a renewable and carbon-neutral resource, with the potential of supplying 14% of the world's energy needs [1].

* Corresponding author, allyon@taltech.ee

The use of biomass as an energy resource can save over one billion tons of CO_2 [2], contributing to the reduction of the environmental impact associated with conventional fossil fuel usage [3, 4]. The high content of volatile matter (60–85 wt%) and low ash content (1–20 wt%) [5, 6] makes biomass types such as woody biomass [7] suitable for producing bio-oil, absorbent materials, and chemical products, among others [8, 9]. Biomass has a biochemical composition of hemicellulose, cellulose, and lignin, components that define its thermochemical behavior, and the yield and quality of products obtained during pyrolysis [10]. An optimal pyrolysis temperature of 520 °C has been identified for achieving the highest yield of bio-oil, resulting in a high yield of liquid and gaseous products (40–70 and 20–30 wt%, respectively) and a low yield of char (10–25 wt%) [11]. At 500–550 °C not only the yields of bio-oil increase, but also the quality, with a lower moisture and oxygen content, and higher heating values, carbon content, and viscosity [12]. The study of bio-oil production is significant in identifying its potential utilization as a fuel or chemical. Bio-oil is dark and viscous, containing a high share of water (15–35 wt%) and a significant share of oxygenated compounds, acids, ethers, and sugars [13]. However, bio-oil is unstable, requiring additional reforming to address its high corrosiveness, chemical instability, and viscosity [14, 15]. The lower toxicity and biodegradability of bio-oil make its potential use as a valuable resource in various applications, including as engine fuel, and in the production of chemicals, such as phenols, resins, and fertilizers.

OS is a non-conventional fossil fuel extracted from geological deposits found in diverse regions worldwide [16]. Notably, its composition is distinguished by a significant proportion of organic material known as kerogen, and a share of inorganic matter and ash. Kerogen, the organic part of OS, can be converted into valuable products, such as shale oil and shale gas, through thermochemical conversion processes [17]. Pyrolysis is usually implemented for OS retorting and the production of shale oil. Typically, OS retorting yields 5–20 wt% of shale oil, 5–20 wt% of shale gas, and >60 wt% of semicoke [18, 19]. Temperatures ranging between 450–550 °C have been proven to yield the highest shares of shale oil [20]; however, the yield and quality of OS pyrolysis depend on the type and composition of OS, the organic matter content and heating value of which can vary from 5 to 80% [21] and from 5 to 20 MJ/kg, respectively. The operational parameters and the type of reactor used also have a direct impact on the yields and quality of the pyrolysis products [22]. The most significant challenges in OS utilization include environmental impacts, such as CO_2, NO_x, and SO_x emissions [23]. Additionally, OS pyrolysis can result in a shale oil with high molecular weight and viscosity, as well as high sulfur content and low stability [23]. As for bio-oil, shale oil may require additional upgrading for its use as a fuel or chemical [24, 25]. The reduction of the yields of solid products (semicoke) is also a challenge to overcome in OS pyrolysis.

Due to the similarity in the operational and thermal conditions required for the degradation of OS and biomass, both fuels can be co-fed in co-pyrolysis to study the thermal degradation and the combined co-pyrolysis properties and yields of the solid, liquid, and gaseous products [26]. The co-pyrolysis of calcium (Ca) rich OS and biomass can potentially result in a more environmentally friendly alternative for the production of energy and chemicals, such as the reduction of emissions from OS utilization, and the use of biomass waste resources [27]. In co-pyrolysis, biomass and OS can interact through chemical reactions or heat transfer mechanisms, resulting in higher yields of products with enhanced properties. Even though biomass and OS pyrolysis occur at the same temperature range [28], the most significant degradation of biomass occurs faster and in a lower temperature region, which can result in heat transfer interactions that enhance OS pyrolysis [29]. Moreover, biomass has a higher hydrogen content, which can act as a hydrogen donor to improve OS thermal cracking and reduce the activation energies of co-pyrolysis blends [30]. Studies on co-pyrolysis of OS and biomass have shown to result in improved properties of solid, liquid, and gaseous products [31, 32] as well as enhanced cracking of fuels and higher product yields [33].

The present study investigated the yields and composition of the products obtained from the intermediate co-pyrolysis of biomass woodchips (WC) and Ca-rich OS in a continuous feed reactor, operating under optimized parameters for the highest yields of liquids at 520 °C in a CO_2 atmosphere. Various blends of OS:WC were pyrolyzed to obtain liquid, gaseous, and solid products. The liquid and solid products were characterized in terms of yields and elemental composition, and a comprehensive physicochemical analysis of the liquid products was conducted, including the measurement of density, viscosity, and the refractive index, Fourier-transform infrared spectroscopy (FTIR), and gas chromatography–mass spectrometry (GC–MS) to identify the most common chemical compounds in the pyrolysis and co-pyrolysis liquids and the functional groups of these compounds. A detailed analysis of the yields and composition of products allowed the identification of the potential benefits of co-pyrolysis, in terms of interactions that can enhance fuel decomposition and product quality, or reduce the environmental impact of conventional retorting processes. The study includes an analysis of GC–MS and FTIR, and characterization of the liquid products to identify the elements and compounds present in individual pyrolysis and co-pyrolysis, which can result in a co-pyrolysis liquid fuel with improved properties. The identification of co-pyrolysis products and their compositions with improved or combined properties highlights the potential of co-pyrolysis as a sustainable and efficient method for biomass and OS valorization.

2. Materials and methods

2.1. Fuel preparation and characterization

Two different fuels were used in pyrolysis and co-pyrolysis: WC and OS. WC consisted of a mix of spruce (*Picea abies*), alder (*Alnus incana*), pine (*Pinus sylvestris*), and birch (*Betula pendula*) from Estonian forests. The OS used is a brown type of OS found in Estonia. The preparation of the fuels consisted of grinding to the required particle size, sieving, drying, and preparing the blends. OS and WC samples were grounded in a Pulverisette 5 ball mill (Laval Lab, Canada) to a particle size below 1 mm, following the ISO 14780:20 standard. The grounded particles were sieved to obtain particle sizes between 0.25 and 1.3 mm, using an Analysette 3 Pro Sieve (Fritsch GmbH, Germany). The sieved particles were dried at 105 °C for 3 h, using a Muffle Furnace L9 (Nabertherm GmbH, Germany) to remove moisture.

WC and OS were characterized in terms of chemical, physical, and thermodynamic properties through elemental analysis, proximate analysis, and calorimetry, respectively. For WC, the elemental analysis was conducted using a Vario MACRO CHNS Cube system (Elementar Analysensysteme GmbH, Germany), according to ISO 16948 and 16994. The proximate analysis to obtain the share of volatile matter, moisture, and ash content was conducted following ISO 18122:2015, 18134:2017, and 18122:2015, respectively. The thermodynamic properties of WC were determined according to ISO 18125, using bomb calorimeters IKA 2000C and IKA 5000C (IKA-Werke GmbH & Co. KG, Germany). Using the abovementioned equipment, the OS elemental analysis was conducted according to ISO 29541:2015, the proximate analysis followed EVS 669:1996 for determining the ash content, and the upper and lower calorific values were determined based on ISO 1928:2016.

Five different samples of WC, OS, and OS:WC blends – OS:WC 7:3, 1:1, and 3:7 – were prepared to obtain samples of 100, 70, 50 and 30 wt% WC, and 100 wt% OS. The blends were manually prepared, using the coning and quartering mixing method, according to ISO 14780:20, and stored in airtight plastic bags, following ISO 14780:20. The prepared mixtures of samples exhibited an average deviation of ±2%.

2.2. Experiment set-up

Pyrolysis and co-pyrolysis of WC, OS, and OS:WC blends were conducted, using a prototype continuous feed reactor. The reactor consists of a retort, a feed hopper, a screw conveyor, a heating system, and a cooling and condensing system. The schematic of the reactor is shown in Figure 1. The continuous feed reactor, where the pyrolysis reactions occur, consists of a cylindrical tank retort, with 85 and 130 mm of diameter and height, respectively, and a capacity of 460 cm^3. The retort is equipped with a cylindrical heater Omega CRFC-46/240-A, 240 V, 900 W (Omega Engineering, Inc., United States), which can heat the reactor to temperatures up to 982 °C. The fuels (WC, OS,

or blends) are stored in feed hopper tanks (560 cm^3) with conical bottoms. These tanks are equipped with agitators to avoid clogging and feed the fuel to the screw feeder. The agitators are powered by electric stepper motors OMC Stepper Online 23HS32-4004S, 48 V, 2.4 Nm, 1.8° step (Stepperonline Inc., United States). From the hopper, the fuel is fed to the screw feeder, driven by the stepper motor (the same type as the one used in the agitator). The fuel is then fed through the screw feeder that discharges the material parallel to the screw axis directly into the retort, providing the screw with greater thrust and preventing blockages.

In the retort, the fuel undergoes a set of chemical reactions at a controlled temperature. The retort is equipped with a supply of carrier gas to prevent air from entering the system and ensure pyrolysis. Additionally, the retort features two cassette heaters IHP 270-08100200, 240 V, 200 W (IHP AB, Sweden) on top of the lid, along with a cartridge heater on the exhaust. These heaters contribute to minimizing condensation at the exhaust and maintaining the desired temperature in the whole retort. The retort's cylindrical heater, along with the cassette and cartridge heaters, is controlled through an Omega CN7523 proportional–integral–derivative (PID) controller (Omega Engineering, Inc., United States), which receives feedback from two TC Direct 405-016 and 405-017 (TC Ltd., United Kingdom) K-type thermocouples. Furthermore, the reactor is equipped with a cooling and condensing system, where the condensable and non-condensable products are cooled down, using a coolant bath, through a Huber TC40E recirculating chiller condensing system (Peter Huber Kältemaschinenbau SE, Germany). This system uses ethylene glycol as a cooling agent that is kept at –30 °C and recirculated through a glass thermosensor containing a finger chiller for oil vapor condensation.

The current research used the continuous feed reactor and fuel blends of OS and WC (OS:WC 0:1, 7:3, 1:1, 3:7, and 1:0) to conduct co-pyrolysis with CO_2 as the carrier gas (50 mL/min) in isothermal conditions at 520 °C. This pyrolysis temperature was chosen as it results in the highest production of liquid products for WC, OS, and OS:WC blends [28]. The cartridge and cassette heaters were also heated to 520 °C. The experiments started when the fuel was fed to the retort from the feed hopper (motor at 10 rpm) to the screw feeder (motor at 5 rpm), with an average feeding rate of 0.05 kg/h for WC, 0.2 kg/h for OS, and 0.05–0.2 kg/h for OS:WC blends. The variable feeding rate was due to the difference in densities, with WC having a lower density than OS. The fuel was fed into the retort for approximately 40–60 min, ensuring sufficient production of liquid products for analysis. Before each experiment, the retort was heated and purged for 30 min with CO_2 to ensure a homogeneous pyrolysis atmosphere, while a leak test was conducted to ensure proper collection of products. After the pyrolysis, the solid products (char, ash, and semicoke) were collected from the cylindrical retort, while the liquid products were collected from the condenser. All components, including the retort, the outlet pipes, and the condenser were weighed both before and

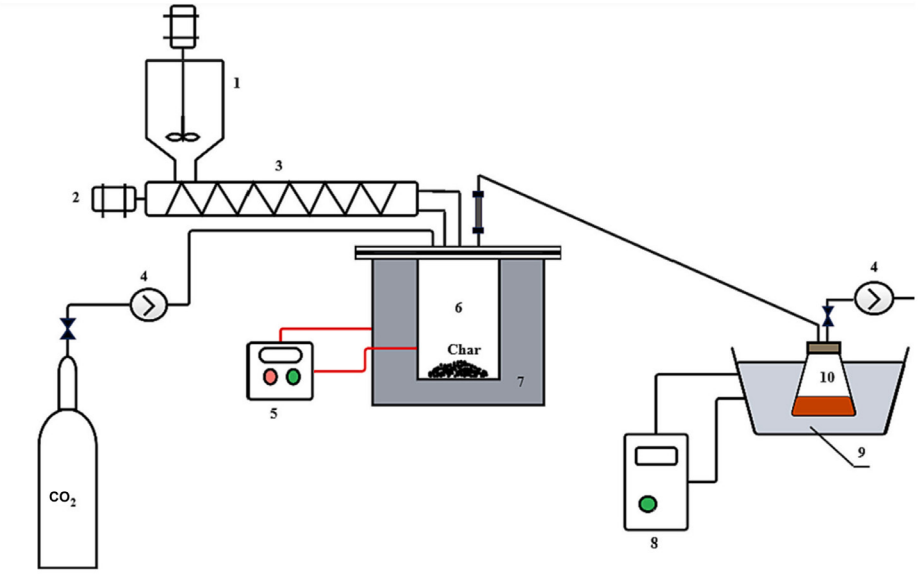

Fig. 1. Schematic of continuous feed reactor [34]: 1 – feed hopper, 2 – stepper motor, 3 – screw feeder, 4 – carrier gas, 5 – PID controller, 6 – retort reactor, 7 – cylindrical heater, 8 – chiller, 9 – coolant bath, 10 – condenser.

after the experiment to obtain a proper mass balance of products. The solid products were stored in airtight bags, and the liquid products were stored in a fridge in airtight containers to prevent evaporation. Each OS:WC blend was pyrolyzed, with two parallel experiments, to ensure low deviation.

The estimated and experimental yields of liquids, solids, and gaseous products from the co-pyrolysis of OS:WC 3:7, 1:1, and 7:3 were derived through the application of a linear correlation involving the shares of OS and WC. This correlation was established based on the experimental yields obtained from individual pyrolysis of both OS and WC, as shown in Equation (1):

$$m_{est} = m_{OS}x + m_{WC}(1–x), \quad (1)$$

where m_{est} is the estimated yields of OS:WC blends, m_{OS} and m_{WC} are the experimental yields, and x is the share of OS.

2.3. Mass balance

For all pyrolysis and co-pyrolysis scenarios, the yields of products were determined by mass balance. At the beginning of the experiment, the initial mass of WC, OS, and OS:WC blends was recorded. The amount of fuel consumed was calculated by the difference between the initial fuel fed and the mass of fuel left in the hopper after the experiment. This amount of fuel

consumed was considered as 100 wt% for calculating the product yields. The yield of solid products was determined by the difference in the initial and final mass of the reactor, as all solid products from pyrolysis remained in the reactor. For liquid products, the yield was calculated using the mass of liquids collected in the condenser (final-initial weight of condenser). Furthermore, the increase of weight in the exhaust pipes and other outlet components was added to the yield of liquids, as these corresponded to condensed deposits on the component's walls. The yield of gas products was calculated by difference, assuming minimal losses due to a low gas flow rate and the leak tests.

2.4. Characterization of solid products

The solid products from the pyrolysis and co-pyrolysis of OS, WC, and OS:WC blends were characterized in terms of elemental composition, proximate composition, and calorific values. The elemental analysis was conducted using a Vario MACRO CHNS Cube system (Elementar Analysensysteme GmbH, Germany), and the calorific values were determined using IKA 2000C and IKA 5000C (IKA-Werke GmbH & Co. KG, Germany).

2.5. Characterization of liquid products

The liquid products were characterized in terms of elemental composition, using a Vario MACRO CHNS Cube system thermal analyzer (Elementar Analysensysteme GmbH, Germany). Additional physicochemical characteristics of the liquid products were measured, including density, viscosity, and the refractive index. The density of the liquid samples was measured at 21°C, using a DMA 5000 M density meter (Anton Paar GmbH, Austria). The viscosity was determined using a MCR 72 modular compact rheometer (Anton Paar GmbH, Austria), with a cone plate spindle at 40 °C. The refractive index was determined using an Abbemat HT refractometer (Anton Paar GmbH, Austria) at a temperature of 20 °C and a wavelength of 589.3 nm. The density, viscosity, and refractive index of water were determined before and after each measurement of oil samples to verify the correct performance of the devices.

2.6. Analysis of liquid products

The liquid samples were analyzed using FTIR and GC–MS. The infrared (IR) spectra of the liquid products from pyrolysis and co-pyrolysis were obtained using an Interspec 301-X portable spectrometer (Interspectrum OÜ, Estonia), with an ATR (attenuated total reflection) in the wavelength ranging from 7000 to 400 cm^{-1}, at a resolution of 1 cm^{-1}, and with an S:N ratio of up to 12000:1. For the pyrolysis liquid products, the samples were analyzed in the wavelength ranging from 600 to 4000 cm^{-1} and at a resolution of 1 cm^{-1}.

The chemical composition of the liquid products of pyrolysis and co-pyrolysis was analyzed with a GC–MS detector to identify different compounds present in the oil. The equipment used was an Agilent 7890B gas

chromatograph (Agilent Technologies, Inc., United States), connected to an Agilent 5975C Inert MSD mass spectrometer (Agilent Technologies, Inc., United States). Helium with a purity of 99.9999% was used as the carrier gas at a flow rate of 0.9 mL/min. The samples were injected using a CTC Combi/GC-PAL 80 autosampler (Agilent Technologies, Inc., United States), with 1 μL of the sample injected with a 10:1 split ratio and an injector temperature of 300 °C. The initial temperature was programmed to start at 40 °C, held for 10 min, followed by a temperature rise to 160 °C with a heating rate of 3 °C/min. The temperature was then raised to 320 °C with a heating rate of 15 °C/min, and kept at 320 °C for 5 min. Each analysis had a total time of 66 min. The liquid products from pyrolysis and co-pyrolysis were analyzed. The GC used a DB-Petro column of 100 m × 250 μm × 0.5 μm. The MS capillary dimensions were 1 m × 250 μm × 0 μm. All the samples were dissolved in acetone, with an average sample concentration of 15 ± 0.8%. Two samples of each pyrolysis oil were measured. The Research Library of the National Institute of Standards and Technology and the Agilent MassHunter Qualitative Analysis Software were used to identify the chromatographic peaks and the compounds. Each sample underwent one more parallel run.

3. Results and discussion

3.1. Fuel properties

The composition of WC and OS in terms of carbon (C), hydrogen (H), nitrogen (N), sulfur (S), oxygen (O), ash and moisture content, fixed carbon, volatile matter, and cross and net calorific values (HHV and LHV, respectively) is shown in Table 1. The WC composition is similar to that of woody biomass species [35], with a high content of C and O, over 80 wt% volatile matter, and low ash content (below 2 wt%). Table 1 displays the composition of the organic part of OS. Compared to WC, OS shows a considerably higher ash content (above 50 wt%), higher density, and lower calorific value. In terms of elemental composition, WC and OS display a significantly different composition, especially of C, H, and O, while OS exhibits a high content of S. The share of volatiles for OS is lower than for WC, which is expected to result in a lower yield of oil and gas products during pyrolysis. Consequently, the pyrolysis behavior and product yields from WC and OS are expected to differ, whereas co-pyrolysis is expected to produce oil, gas, and char with additive product yields [36].

Table 1. Properties of woodchips and oil shale

Composition		Woodchips	Oil shale
Elemental analysis, wt%	C	51.68	27.00
	H	6.44	2.46
	N	0.35	0.06
	S	<0.10	1.65
	O*	41.53	15.40
Proximate analysis, wt%	Ash content	1.54	51.42
	Moisture	6.40	0.90
	Fixed carbon*	10.58	1.48
	Volatile matter	81.48	47.10
Calorific value, MJ/kg	LHV	18.76	8.72
	HHV	20.16	9.73

* Calculated

3.2. Pyrolysis and co-pyrolysis yields

The yields of gas, solid, and liquid products from the pyrolysis and co-pyrolysis of OS and WC at 520 °C are illustrated in Figure 2. The measured yields of liquid and solid products exhibit a relative standard deviation of 1.43–6.88% and 3.41–8.73% for each parameter and its replicates, respectively. As expected, WC yields a higher share of gas and liquid products, with 43.9 wt% for liquids (oil + water), 35.1 wt% for gas, and 21.0 wt% for solids, primarily composed of pyrolysis char. These product yields are consistent with the expected yields of woody biomass in intermediate pyrolysis [6, 10, 11, 37], as also observed in studies of various types of woody biomass (Table 2). Comparison of the current study with the studies displayed in Table 2 reveals that the obtained product yields closely match those reported in other studies of intermediate pyrolysis at 450–650 °C, with average product yields of 35–62 wt% for liquids, 22–41 wt% for gas, and 21–37 wt% for solids. A higher yield of liquids and gas, coupled with a lower yield of solids (21.0 wt%), indicates that the pyrolysis was complete, based on the elemental composition in Table 1, with a low share of unreacted fuel.

OS yielded a higher share of solid products (74.3 wt%), and lower yields of liquid (17.3 wt%) and gas products (8.4 wt%). The higher yield of solids is due to the considerably higher ash content in OS compared to WC, as shown in Table 1. The lower volatile content of OS results in lower yields of liquid

and gas products. The pyrolysis yields of OS are consistent with the expected pyrolysis yields of OS, including 5–20 wt% for liquids (shale oil), 5–20 wt% for gas (shale gas), and >60 wt% for solids (semicoke) [22]. Table 3 shows a comparison of product yields from pyrolysis at 420–600 °C of diverse types of OS. The product yields from OS pyrolysis closely match with the yields obtained in other studies, with 7–46 wt% for liquids, 5–31 wt% for gas, and 37–76 wt% for solids. The wide range of product yields observed in the comparative analysis in Table 3 can be attributed to the different types of OS used, which contain different shares of organic matter. The OS used in the current study yielded 74.3 wt% for solids due to the higher ash content of the fuel. This share of solids consists of semicoke, which is composed of ash and organic matter that did not pyrolyze [18, 19].

Figure 2 displays the yields of co-pyrolysis products from OS:WC 7:3, 1:1, and 3:7. There is an evident additive relation between the product yields and the blend ratio of OS:WC. The yields of liquids rise as the share of WC increases, starting at 17.3 wt% for OS:WC 1:0 and rising to 22.2, 26.9, 33.1, and 43.9 wt% for OS:WC 7:3, 1:1, 3:7, and 0:1, respectively. The case is similar for gas products, starting at 8.4 wt% for OS:WC 1:0 and rising to 22.7, 26.8, 30.3, and 35.1 wt% for OS:WC 7:3, 1:1, 3:7, and 0:1, respectively. On the other hand, the yields of solid products decrease as the share of WC raises: OS:WC 1:0 yields 74.4 wt% of solids, while the yield decreases to 55.1, 46.3, 36.6, and 21.0 for OS:WC 7:3, 1:1, 3:7, and 0:1, respectively. The product yields from co-pyrolysis indicate a linear behavior as the ratio of WC increases, demonstrating a linear increase in liquid yields with a coefficient of determination R^2 of 0.9704, and a linear decrease in solid yields with an R^2 of 0.9955.

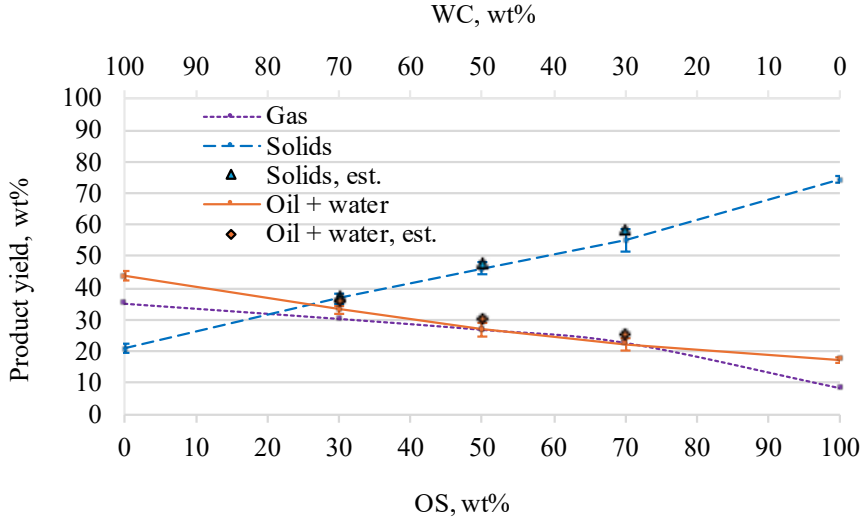

Fig. 2. Experimental and estimated (est.) product yields from the co-pyrolysis of oil shale and woodchips.

Table 2. Comparative analysis of woody biomass yields from intermediate pyrolysis

Biomass type	Experiment type	Operating temperature, °C	Residence time, min	Particle size, mm	Liquid yield (oil + water), wt%	Gas yield, wt%	Solid yield, wt%
Woodchips, current study	**Continuous feed reactor**	**520**	**40–60**	**0.25–1**	**44**	**35**	**21**
Pine sawdust [38]	Fixed bed reactor	550	30	1	45	26	28
Paulonwnia wood [39]	Fixed bed reactor	500	–	0.22–0.42 0.42–1.1 1.1–1.8	25–30	22–27	26
Beech and spruce [40]	Tubular reactor	427	–	1.0–2.5	36–38	–	34–37
Beech and pine pellets [41]	Stainless steel capsule	670–970	25	11–13 diameter 60 length	53–62	17–21	21–27
Pinewood [42]	Rotary kiln reactor	500	30	4	35	41	24
Spruce and pine sawdust [43]	Furnace	500	–	0.5–2	50	25	25
Pine sawdust [44]	Screw reactor	600	6	1–2	52	22	20
Spruce [45]	Cylindrical reactor	525	–	–	45	30–35	28
Silver birch [46]	Batch retort	450	–	–	38–43	18–22	34

Table 3. Comparative analysis of yields of oil shale pyrolysis

Oil shale	Experiment type	Operating temperature, °C	Residence time, min	Particle size, mm	Liquid yield (oil + water), wt%	Gas yield, wt%	Solid yield, wt%
Oil shale, current study	**Continuous feed reactor**	**520**	**40–60**	**0.25–1**	**17**	**8**	**74**
Göynük [47]	Autoclave	420	120	<0.12	37–46	10–16	37–52
Huadian [33]	Retorting reactor	490–590	–	<0.9	7–19	15–20	65–76
Huadian [31]	Cylindrical retort	520	20	<3	32	5	66
Huadian [28]	Bubbling fluidized bed reactor	430–600	–	3	21	13	67
Kukersite [22]	Fischer assay	520	–	0.04–0.1	34	8	58
Göynük [48]	Fixed bed reactor	600	60	1	30	32	38

Figure 2 also shows a comparison between the experimental and estimated yields of co-pyrolysis products based on Equation (1). Overall, the experimental yields for solid and liquid products were lower than the estimated yields. The latter were 0.4–3.7 wt% higher, suggesting some interactions between the fuels during co-pyrolysis. However, considering the deviation of up to 9% between parallel experiments and the ±2 wt% sample mixing deviation, the difference between experimental and estimated yields is in all likelihood due to experimental uncertainties, including the collection of liquid and solid products.

The product yields from co-pyrolysis follow an additive linear relation, with increases in liquid and gas yields and decreases in solid product yields as the share of WC rises. Other studies have also observed additive behavior and low or no interactions [24, 47, 49] during the co-pyrolysis of OS and biomass. However, the addition of WC to OS improved the pyrolysis process, resulting in reduced solid product yields and increased oil and gas yields [31, 32, 50]. WC pyrolysis starts at a lower temperature region due to its biochemical composition [10]; therefore, the resulting products may interact with OS through heat transfer or chemical reactions, enhancing the pyrolysis

process for OS. Additionally, the higher H content of WC (Table 1) and alkali and alkaline earth metals [33] can promote the decomposition of OS through a catalytic effect [32, 33, 51, 52].

3.3. Solid products

The characteristics of the solid products from OS and WC pyrolysis and co-pyrolysis are shown in Table 4. The elemental composition, proximate composition, and calorific values exhibit relative standard deviations of 0.21–10.28%, 0.12–6.72%, and 1.00–6.31% for each parameter and its replicates, respectively. Experimental analysis of solid products reveals an increase in C and H content and calorific values of OS:WC blends as the share of WC rises. On the other hand, S and ash contents decrease as the share of WC rises. Solid products from WC pyrolysis mostly consist of char (81.1 wt% C), with ash content below 8 wt%, which agrees with the composition of char from the intermediate pyrolysis of woody biomass [53, 54]. Solid products from OS pyrolysis mostly comprise ash (67.7 wt%) and a low fraction of char (below 13 wt%), which agrees with the semicoke composition from OS pyrolysis [55]. Solid products from OS:WC blends have compositions between those of WC and OS. The volatile matter in the chars indicates incomplete degradation during pyrolysis and co-pyrolysis [44] for blends containing shares of OS. The addition of WC to OS in co-pyrolysis contributes to solid products with

Table 4. Composition of solid products from the pyrolysis and co-pyrolysis of oil shale and woodchips

	OS:WC blend	WC	3:7	1:1	7:3	OS
Elemental analysis, wt%	C	81.10	31.74	23.26	18.76	12.90
	H	3.12	1.08	0.70	0.50	0.28
	N	0.58	0.19	0.11	0.08	0.04
	S	0.15	1.13	1.32	1.36	1.53
Proximate analysis, wt%	Ash content	7.44	49.86	58.09	62.1	67.74
	Moisture	11.41	5.54	2.93	1.73	0.73
	Fixed carbon*	62.45	15.00	10.17	9.50	5.32
	Volatile matter	18.70	29.59	28.81	26.67	26.21
Calorific value, MJ/kg	LHV	29.54	9.07	5.66	3.84	1.89
	HHV	30.23	9.31	5.82	3.96	1.96

* Calculated

higher calorific values, higher C and H contents, and lower ash and S contents. These properties result in an improved char with enhanced thermal properties; for example, higher C and H contents increase the heating value of char, while lower ash and S contents decrease possible environmental effects of using the solid products from the co-pyrolysis of OS and WC. According to literature, the chars obtained from the co-pyrolysis of WC, OS, and OS:WC at 520 °C have higher aromaticity and thus higher stability, rendering them suitable for applications such as absorbent materials, pollutant sorbents, and bio-char [13, 56], especially for chars from WC and OS:WC blends with high shares of WC.

3.4. Characterization of liquid products

Table 5 summarizes the properties of the raw liquid products from the pyrolysis and co-pyrolysis of OS, WC, and OS:WC blends, with a relative standard deviation for viscosity, density, refractive index, and elemental composition of 6.35–11.51%, 0.37–0.67%, 0.18–0.35%, and 1.07–10.10% for each parameter and its replicates, respectively.

The pyrolysis oil derived from WC (OS:WC 0:1) is viscous, dense, and of brown color, with a characteristic pungent-like barbecue odor [57]. In the pyrolysis with 100 wt% WC, the composition of the liquid part agrees with the typical composition of pyrolysis liquids from woody biomass, with C, H, and N ranging from 54.0–58.0, 5.5–7.0, and 0.0–0.2 wt%, respectively [58]. A higher share of H (8.85 wt%) observed in this study may be due to greater water content in the liquid part, which can reach up to 35 wt% [13]. The physicochemical properties of the liquid products from WC are also in agreement with other studies, with reported viscosity values ranging from 40–100 mPa·s, and densities of 1.0–1.2 kg/m^3 [45, 57, 59, 60]. The relatively high viscosity of bio-oil can be attributed to the high molecular weight of the lignin-derived compounds, potentially affecting bio-oil operating temperatures, as well as combustion efficiency, and emissions [45]. Furthermore, the density of bio-oil is also relatively higher compared to conventional liquid fuels [58]. As with all bio-oils, the current bio-oil requires upgrading and refining [58].

The pyrolysis oil derived from OS (OS:WC 1:0) is lighter and of dark brown color. Pyrolysis of 100 wt% OS resulted in elemental composition and physicochemical properties comparable to those reported in other studies, with C, H, and N contents falling within the ranges of 78–82, 9–11, and 0.03–2.2 wt%, respectively [23, 61, 62]. While the content of S in shale oil is relatively high compared to that in bio-oil, it is comparable to or lower than the content of S in most crude oils (0.01–4.20 wt%). The shale oil obtained exhibits a higher carbon/hydrogen (C/H) ratio than crude oil (5.28–7.73). Even though the difference is not significant, it causes fouling during processing [23, 58]. The density, viscosity, and refractive index of OS are also in agreement with literature findings, with observed densities ranging between 0.89–0.99 g/cm^3 [62, 63]. These characteristics indicate that the shale oil analyzed possesses lower density and viscosity compared to petroleum-derived oils [58].

Table 5. Composition of liquid products from the pyrolysis and co-pyrolysis of oil shale and woodchips

OS:WC blend		WC	3:7	1:1	7:3	OS
Viscosity, mPa·s		51.08	38.79	29.5	17.28	12.30
Density, g/cm^3		1.06	1.05	1.02	1.01	0.95
Refractive index, n.D*		1.52	1.54	1.54	1.53	1.53
Elemental analysis, wt%	C	58.52	68.27	65.79	78.74	80.64
	H	8.85	8.82	8.48	9.40	9.25
	N	0.35	0.32	0.32	0.28	0.17
	S	0.33	0.43	0.71	0.82	0.85
C/H ratio		6.62	7.74	7.76	8.38	8.72

* n.D – dimensionless

The characteristics of the liquids obtained from the co-pyrolysis of OS and WC (OS:WC 3:7, 1:1, and 7:3) range between those obtained from the individual pyrolysis of OS and WC. The co-pyrolysis of OS and WC also results in oils with enhanced properties. The oil blends of OS:WC exhibit reduced S content (0.43–0.82 wt%) and a lower C/H ratio (7.74–8.38) due to the WC properties, while demonstrating a higher content of C (58.52–78.74 wt%), along with lower viscosity (17.28–38.79 mPa·s) and density (1.01–1.05 g/cm^3). These combined properties facilitate the production of pyrolysis oil with properties more similar to those of conventional petroleum-derived oils. The refractive index remains almost the same for all OS:WC blends (1.52–1.54).

3.5. Analysis of liquid products

3.5.1. GC–MS analysis

The GC–MS spectra were obtained for the liquid products from the pyrolysis and co-pyrolysis of OS, WC, and OS:WC blends. The chromatograms obtained using Agilent MassHunter Qualitative Analysis Software are shown in Figure 3, indicating the identified peaks, their abundance, and retention times. At first glance, there is an evident difference between the chromatograms of WC and OS pyrolysis liquid products, with larger peaks for WC at lower retention times (15–25 min) and for OS at higher retention times (30–50 min). The chromatograms of co-pyrolysis liquid products OS:WC 3:7, 1:1, and 7:3 indicate a combination of the OS and WC chromatograms.

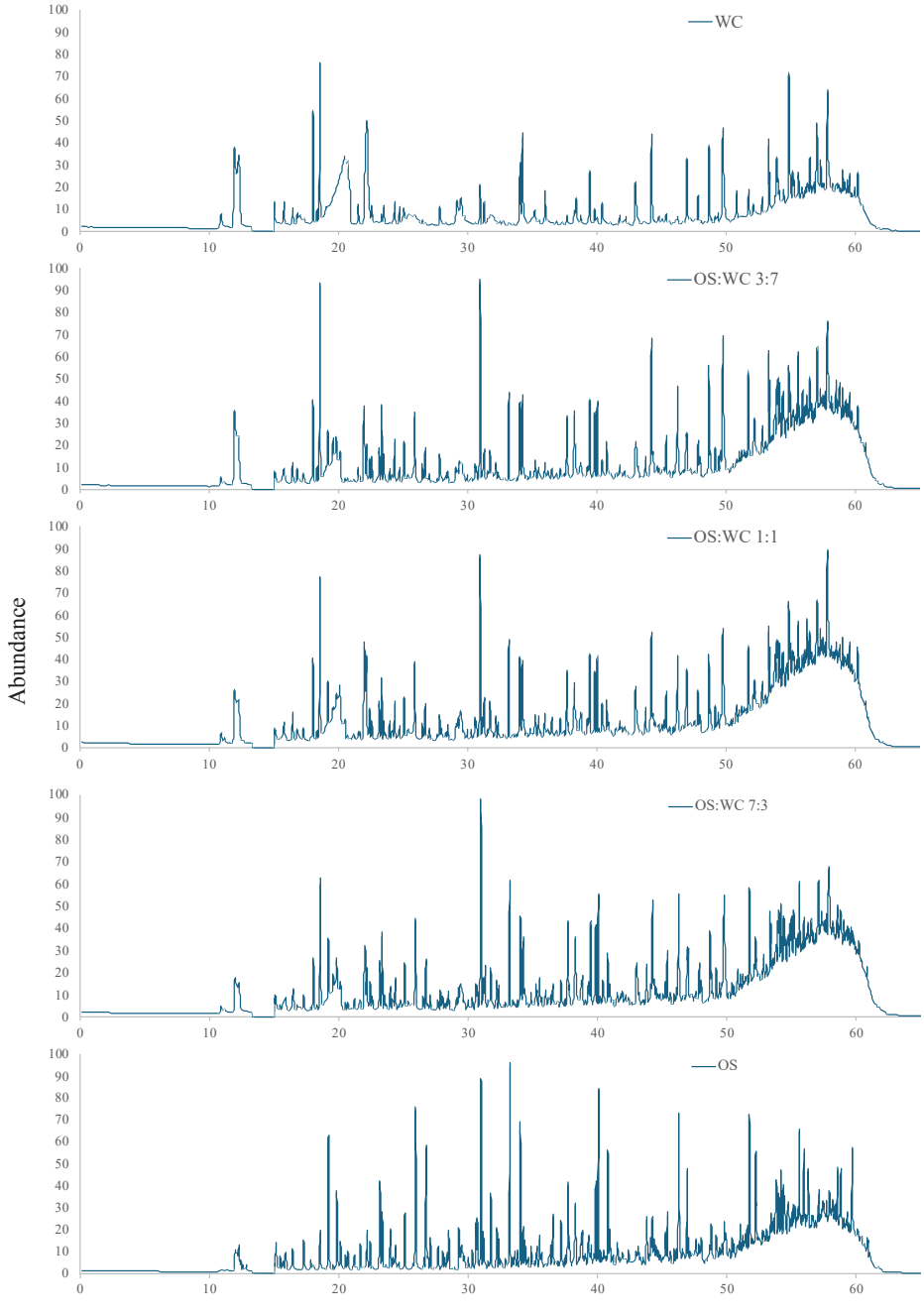

Fig. 3. GC–MS chromatogram of liquid products from the pyrolysis of WC, OS and OS:WC blends 7:3, 1:1 and 3:7.

Based on the observations, a qualitative analysis was conducted, using the compounds identified by the Research Library of the National Institute of Standards and Technology. The selection of the compounds was based on the score given by the Agilent MassHunter Qualitative Analysis Software, which is based on the coelution score, calculated based on abundance, peak symmetry, width, and retention time. Compounds with a score above 70 were selected, resulting in average scores of 84.6, 80.2, 78.8, 79.3, and 83.3 for OS:WC 0:1, 3:7, 1:1, 7:3, and 1:0, respectively. Based on a comparison of the scores obtained, and a comparison of the parallel runs of liquid products analysis, compounds with high scores detected in both parallel measurements were selected for qualitative analysis. As a result, 21, 25, 30, 39, and 42 compounds were identified in OS:WC 0:1, 3:7, 1:1, 7:3, and 1:0, respectively. It was immediately observed that OS:WC ratios with higher OS shares had more compounds identified. For all OS:WC ratios, the identified compounds with their chemical formulae were organized by abundance and retention time (Figs 4, 5).

Figure 4 displays the identified compounds for the WC liquid products. Overall, these compounds belong to the functional groups of ketones, carboxylic acids, siloxanes, aromatic hydrocarbons, aldehydes, phenols, and dihydrobenzenes. Ketones (C=O) and phenols (OH) were the most common groups identified. From the ketone functional group, some compounds identified include 2-butanone and cyclic ketones. From the phenol functional group, the compounds identified include phenol, phenol with 2-methyl, and phenol with ethyl. Other identified compounds include benzenediols, esters, carboxylic acids, and aldehydes. From the chromatogram of WC, only one aromatic hydrocarbon – toluene – was identified. In the WC liquid products, most compounds were oxygen-containing compounds, with relatively small numbers of carbon atoms, from C_2 to C_8. The characterization obtained from the GC–MS spectra of the WC liquid products agrees with other studies, which have also reported a large number of phenols and ketones [38, 64], low molecular-weight oxygenated organic compounds [39, 65–67], and less acidic compounds [68]. However, studies by Yorgun and Yıldız [39] and Sugumaran et al. [69] identified phenols and ketones, as well as aliphatic and aromatic hydrocarbons, such as heavier alkanes and alkenes C_{14} to C_{20}, which were not identified in the WC liquid products in the current study. These compounds identified in WC, including cyclic ketones and phenols with multiple substituents, benzenediols, esters, and carboxylic acids, contribute to challenges in refining and utilizing the bio-oil. Additionally, the predominance of oxygen-containing compounds may reduce the energy density and overall efficiency as a fuel.

The compounds identified in the OS liquid products (Fig. 4) are significantly different than those in the WC liquid products. These compounds belong to functional groups including aromatic hydrocarbons, aliphatic hydrocarbons, aliphatic alcohols, cycloalkanes, polycyclic compounds, phenols, and

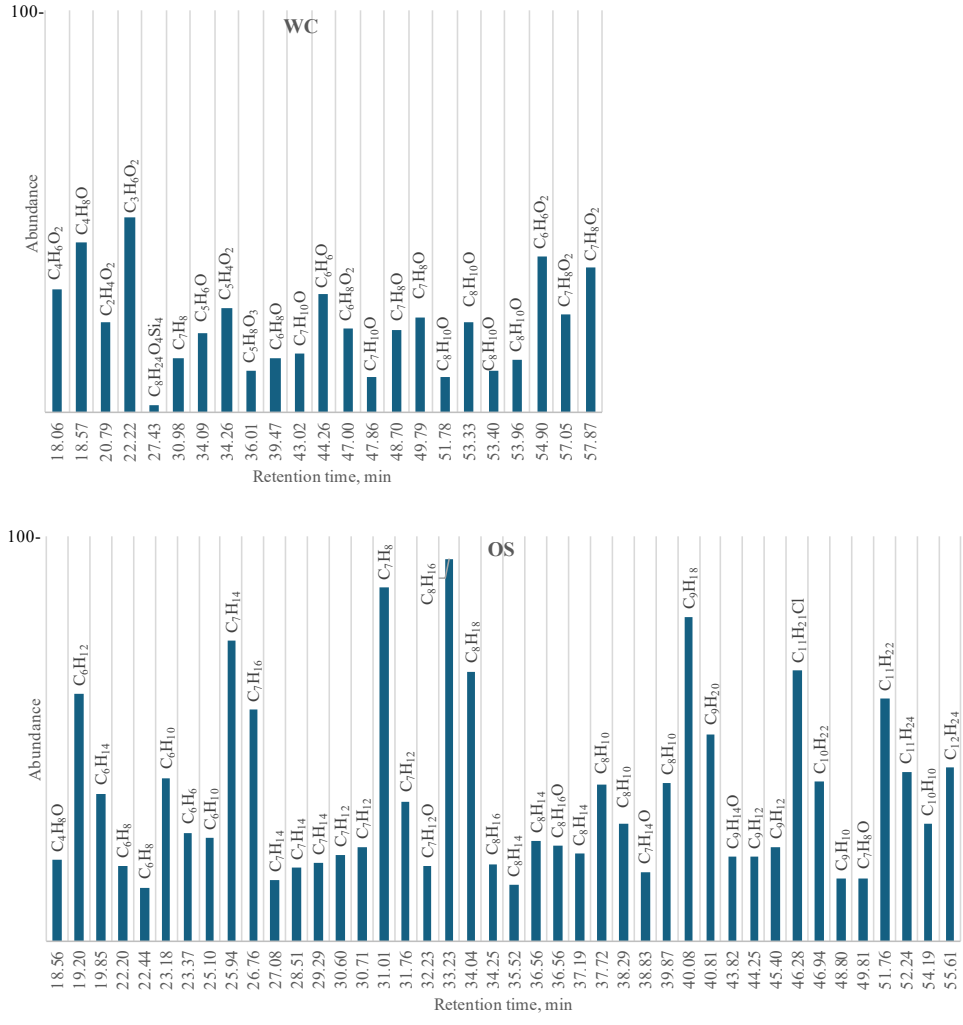

Fig. 4. Most abundant compounds in the liquid products from the pyrolysis of oil shale and woodchips.

ketones. Most compounds present in the OS liquid products were aromatic hydrocarbons, aliphatic hydrocarbons, and cycloalkanes. Among these, the most abundant were aliphatic hydrocarbons, including alkenes, alkanes, and alkynes, ranging from C_6 to C_{11}. Some aromatic hydrocarbons, such as benzene, toluene, and o-Xylene, ranging from C_6 to C_{11}, were found too. Additionally, various cycloalkanes, ranging from C_6 to C_{12}, were identified. Although fewer in number, some oxygen-containing compounds, such as ketones, phenols, polycyclic compounds, and aliphatic alcohols, were also identified.

Compared to WC liquid products, the OS liquid products were mostly composed of compounds with a larger number of carbon atoms, from C_4 to C_{12},

heavier aromatic and aliphatic hydrocarbons, both cycloalkanes and alkenes, and less oxygen-containing compounds. The functional groups identified in the liquid products of OS pyrolysis agree with other studies, with the presence of larger chains [24] of aliphatic and aromatic hydrocarbons, including alkenes and alkanes [61], and monocyclic and polycyclic hydrocarbons [47]. Similar to the current study, Jiang et al. [33] found a large proportion of aliphatic hydrocarbons. The abundant aliphatic hydrocarbons, including alkenes, alkanes, and alkynes, are an advantage of the shale oil obtained, with great potential for liquid fuel applications. Their high energy density and compatibility with existing infrastructure make shale oil a candidate for meeting energy demands. Moreover, the presence of cycloalkanes enhances its suitability for refinement into valuable liquid fuels.

The compounds identified in the liquid products from the co-pyrolysis of OS:WC 3:7, 1:1, and 7:3 are shown in Figure 5. These liquid products were mostly composed of compounds from the same functional groups identified in the individual pyrolysis of OS and WC, such as ketones, carboxylic acids, siloxanes, aromatic hydrocarbons, aliphatic hydrocarbons, aldehydes, phenols, and aromatic carboxylic acids. All OS:WC blends containing WC had the same types of compounds identified in the ketones and phenols functional groups, including 2-butanone, ketones with hydroxyl, cyclic ketones, phenols, phenols with methyl, and phenols with ethyl. As the OS ratio increased, the amount of aromatic and aliphatic hydrocarbons also increased. Among the aromatic hydrocarbons, the identified compounds ranging from C_6 to C_{11} included benzene, ethyl, and methyl with benzene rings and o-Xylene. The identified aliphatic hydrocarbons, ranging from C_7 to C_{11}, included alkenes, alkanes, and alkynes, as well as methyl group alkanes. A comparison of the functional group distribution of the compounds identified in the liquid products from the OS:WC blends is shown in Table 6.

As evident in Table 6, the co-pyrolysis of OS and WC yielded liquid products containing compounds from both OS and WC: mostly ketones and phenols from WC, and aliphatic and aromatic hydrocarbons from OS. Based on this composition, and the yields and compositions of the liquid products shown in Figure 2 and Table 5, the co-pyrolysis products appear to be a result of an additive mixture from OS and WC, rather than any synergistic promoting or inhibiting effects. This has also been observed in the co-pyrolysis of *Euphorbia rigida* and OS, where the co-pyrolysis liquid products contained oxygenated and acid-based compounds produced from *Euphorbia rigida*, and hydrocarbons from OS [24]. The co-pyrolysis of OS and terebinth berries identified a higher share of polycyclic and monocyclic hydrocarbons in OS products than in terebinth berries' products, resulting in an additive composition for the co-pyrolysis liquid products.

Despite the lack of synergistic effects, the co-pyrolysis results in improved liquid products. From the WC side, the addition of OS reduces the production of ketones, which are considered undesirable due to their low stability and

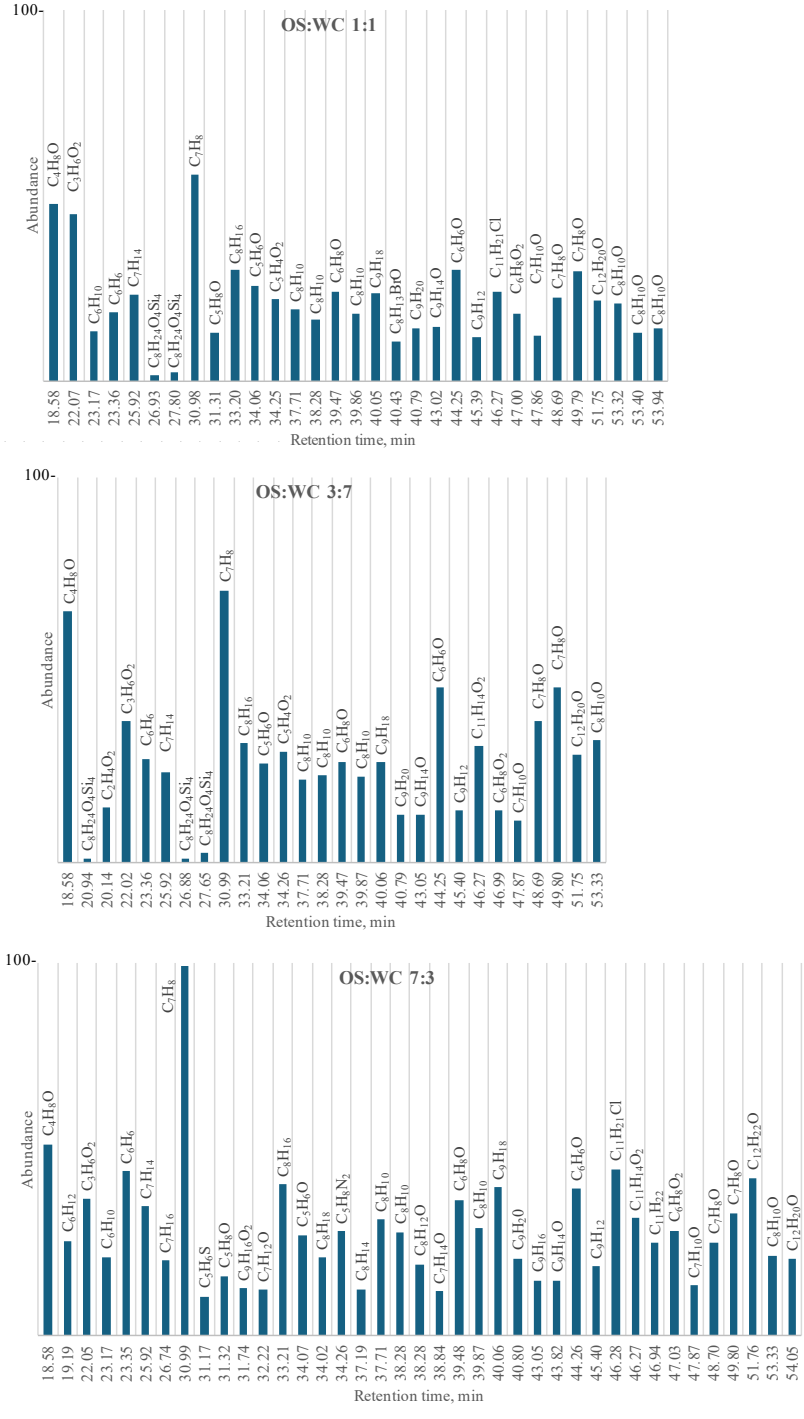

Fig. 5. Most abundant compounds in the liquid products from the co-pyrolysis of OS:WC 3:7, 1:1, and 7:3.

Table 6. Comparison of functional group distribution in the liquid products from the pyrolysis and co-pyrolysis of oil shale and woodchips

Functional group	WC	OS:WC 3:7	OS:WC 1:1	OS:WC 7:3	OS
Ketones	8	7	7	6	2
Aromatic hydrocarbons	1	7	9	9	10
Aliphatic hydrocarbons	0	5	6	9	19
Phenols	8	6	6	6	1

heating value [33]. Conversely, the addition of WC to OS decreases aromatic hydrocarbons. The higher number of oxygenated compounds in WC liquid products is also explained by the larger content of oxygen in WC compared to OS, as shown in the elemental composition (Table 1), while the greater amount of hydrocarbons detected in the OS liquid products can be due to the higher content of oxygen and hydrogen in the OS liquids (Table 4).

The co-pyrolysis of OS and WC presents an opportunity to make use of the favorable properties of shale oil to enhance the quality of bio-oil. By combining OS and WC, the resulting liquid products benefit from the composition of shale oil, characterized by its abundance of aliphatic hydrocarbons that contribute to the improved properties of the co-pyrolysis liquid products, offering higher energy density, improved stability, and enhanced suitability for various applications, including liquid fuels. The addition of OS to the co-pyrolysis process decreases the presence of oxygenated compounds (with low stability and heating value), thus enhancing the overall quality of the resulting co-pyrolysis oil. Moreover, the reduction in aromatic hydrocarbons present in shale oil further improves the liquid products, reducing pollutants caused by the combustion of aromatic hydrocarbons.

3.5.2. FTIR analysis

The FTIR spectra of the pyrolysis and co-pyrolysis products of OS and WC are shown in Figure 6. These spectra are divided by wavenumber sections, which indicate the presence of different functional groups. The wavenumber ranges between 3200–3600 cm^{-1}, caused by O–H stretching vibrations indicating the presence of phenols, alcohols, and other OH functional groups. Aliphatic hydrocarbons such as alkanes are identified by C–H stretching vibrations in the range of 2800–3000 cm^{-1}, and C–H bending in the range of 1325–1490 cm^{-1}. The peaks within the range of 1650–1775 cm^{-1} indicate C=O stretching vibrations from ketones, esters, and carboxylic acids, while the range of 1575–1680 cm^{-1} identifies alkenes with C=O stretching. The lower range of 950–1300 cm^{-1} indicates C–O stretching vibrations from alcohols and phenols.

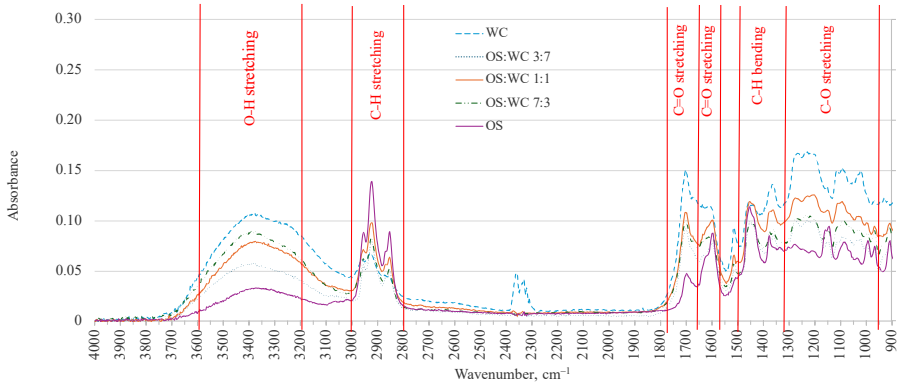

Fig. 6. Infrared spectra of the liquid products from the pyrolysis and co-pyrolysis of OS and WC.

Similar to the results obtained from the GC–MS analysis, the IR spectra show clear differences between the WC and OS liquid products due to the diverse types of compounds produced in the individual pyrolysis of each fuel. The IR spectra are in agreement with the GC–MS results. For the WC liquid products, the IR peaks are stronger within the ranges of 950–1300, 1650–1775, and 3200–3600 cm^{-1} due to the larger presence of oxygenated compounds, phenols, and ketones. On the other hand, the IR spectra of the OS liquid products resulted in larger peaks in the 2800–3000 cm^{-1} range, and more bent peaks in the 1325–1490 cm^{-1} range, reflecting the greater presence of aliphatic hydrocarbons, as also detected by GC–MS.

The co-pyrolysis liquid products resulted in the IR spectra with combined characteristics and peaks from the spectra of OS and WC, reiterating the additive behavior of OS and WC co-pyrolysis. Similar results for the IR spectra are reported by Kiliç et al. [24] and Jiang et al. [33] for OS and biomass co-pyrolysis, and Mozaffari et al. [62] for shale oil pyrolysis.

Conclusions

This study analyzed the yield and composition of the products from the co-pyrolysis of oil shale and woodchips. The elemental composition of the fuel, solid and liquid products, as well as the functional groups, most relevant organic compounds, and the physicochemical properties of the liquid fraction were analyzed using GC–MS, FTIR, and other analytical equipment.

1. The product yields and elemental composition of the liquid and solid products demonstrated an additive behavior in co-pyrolysis, with no synergistic or inhibiting effects in co-pyrolysis. The functional groups present in the co-pyrolysis liquid products corroborated the additive behavior, with oxygenated compounds derived from biomass bio-oil, and aromatic and aliphatic hydrocarbons derived from shale oil.

2. The liquid products obtained from biomass pyrolysis were composed of oxygenated compounds such as ketones and phenols, while shale oil consisted of aromatic and aliphatic hydrocarbons, and cycloalkanes. The co-pyrolysis liquid products were composed of an additive mixture of bio-oil and shale oil compounds. The addition of oil shale to biomass resulted in a reduction in oxygenated compounds, while the addition of biomass to oil shale led to a decrease in aromatic compounds. Thus, the liquid product demonstrated enhanced properties, such as higher stability and heating value, rendering it suitable for potential use as a fuel or chemical.
3. Future research could involve exploring variations in process parameters such as temperature, residence time, and catalyst usage. Additionally, conducting detailed quantitative analyses of the composition of both the liquid and gaseous products could provide deeper insights. Economic and environmental assessments could help evaluate the feasibility and sustainability of scaling up co-pyrolysis of oil shale and biomass for commercial applications.

Acknowledgments

This article was supported by the European Regional Development Fund and the Estonian Research Council (grant PSG266). The authors are grateful to the peer reviewers for their constructive feedback. The publication costs of the article were covered by the Estonian Academy of Sciences.

References

1. Mehmood, M. A., Ye, G., Luo, H., Liu, C., Malik, S., Afzal, I., Xu, J., Ahmad, M. S. Pyrolysis and kinetic analyses of Camel grass (*Cymbopogon schoenanthus*) for bioenergy. *Bioresour. Technol.*, 2017, **228**, 18–24. https://doi.org/10.1016/j.biortech.2016.12.096
2. Antar, M., Lyu, D., Nazari, M., Shah, A., Zhou, X., Smith, D. L. Biomass for a sustainable bioeconomy: an overview of world biomass production and utilization. *Renew. Sustain. Energy Rev.*, 2021, **139**, 110691. https://doi.org/10.1016/j.rser.2020.110691
3. Erkiaga, A., Lopez, G., Amutio, M., Bilbao, J., Olazar M. Influence of operating conditions on the steam gasification of biomass in a conical spouted bed reactor. *Chem. Eng. J.*, 2014, **237**, 259–267. https://doi.org/10.1016/j.cej.2013.10.018
4. Van de Velden, M., Baeyens, J., Brems, A., Janssens, B., Dewil, R. Fundamentals, kinetics and endothermicity of the biomass pyrolysis reaction. *Renew. Energy*, 2010, **35**(1), 232–242. https://doi.org/10.1016/j.renene.2009.04.019
5. Wang, X., Deng, S., Tan, H., Adeosun, A., Vujanović, M., Yang, F., Duić, N. Synergetic effect of sewage sludge and biomass co-pyrolysis: a combined study

in thermogravimetric analyzer and a fixed bed reactor. *Energy Convers. Manag.*, 2016, **118**, 399–405. https://doi.org/10.1016/j.enconman.2016.04.014
6. Zhang, L., Xu, C. (Charles), Champagne, P. Overview of recent advances in thermo-chemical conversion of biomass. *Energy Convers. Manag.*, 2010, **51**(5), 969–982. https://doi.org/10.1016/j.enconman.2009.11.038
7. Smołka-Danielowska, D., Jabłońska, M. Chemical and mineral composition of ashes from wood biomass combustion in domestic wood-fired furnaces. *Int. J. Environ. Sci. Technol.*, 2022, **19**(6), 5359–5372. https://doi.org/10.1007/S13762-021-03506-9
8. Demirbas, M. F., Balat, M. Recent advances on the production and utilization trends of bio-fuels: a global perspective. *Energy Convers. Manag.*, 2006, **47**(15–16), 2371–2381. https://doi.org/10.1016/j.enconman.2005.11.014
9. Singh, R. K., Ruj, B. Time and temperature depended fuel gas generation from pyrolysis of real world municipal plastic waste. *Fuel*, 2016, **174**, 164–171. https://doi.org/10.1016/j.fuel.2016.01.049
10. Wang, S., Luo, Z. *Pyrolysis of Biomass*. De Gruyter, Berlin, Boston, 2017. https://doi.org/10.1515/9783110369632-001
11. Uddin, M. N., Techato, K., Taweekun, J., Rahman, M. M., Rasul, M. G., Mahlia, T. M. I., Ashrafur, S. M. An overview of recent developments in biomass pyrolysis technologies. *Energies*, 2018, **11**(11), 3115. https://doi.org/10.3390/en11113115
12. Garcia-Perez, M., Wang, X. S., Shen, J., Rhodes, M. J., Tian, F., Lee, W. J., Wu, H., Li, C. Z. Fast pyrolysis of oil mallee woody biomass: effect of temperature on the yield and quality of pyrolysis products. *Ind. Eng. Chem. Res.*, 2008, **47**(6), 1846–1854. https://doi.org/10.1021/ie071497p
13. Igliński, B., Kujawski, W., Kiełkowska, U. Pyrolysis of waste biomass: technical and process achievements, and future development – a review. *Energies*, 2023, **16**(4), 1829. https://doi.org/10.3390/en16041829
14. Wang, Q., Li, X., Wang, K., Zhu, Y., Wang, S. Commercialization and challenges for the next generation of biofuels: biomass fast pyrolysis. In: *2010 Asia-Pacific Power and Energy Engineering Conference*, March 28–30, 2010, IEEE, 2010, 1–4. https://doi.org/10.1109/APPEEC.2010.5448437
15. Sharifzadeh, M., Sadeqzadeh, M., Guo, M., Borhani, T. N., Murthy Konda, N. V. S. N., Garcia, M. C., Wang, L., Hallett, J., Shah, N. The multi-scale challenges of biomass fast pyrolysis and bio-oil upgrading: review of the state of art and future research directions. *Prog. Energy Combust. Sci.*, 2019, **71**, 1–80. https://doi.org/10.1016/j.pecs.2018.10.006
16. EIA (U.S. Energy Information Administration). *Technically Recoverable Shale Oil and Shale Gas Resources: An Assessment of 137 Shale Formations in 41 Countries Outside the United States*, EIA, 2013.
17. Foltin, J. P., Lisboa, A. C. L., de Klerk, A. Oil shale pyrolysis: conversion dependence of kinetic parameters. *Energy Fuels*, 2017, **31**(7), 6766–6776. https://doi.org/10.1021/acs.energyfuels.7b00578
18. Boak, J. Shale-hosted hydrocarbons and hydraulic fracturing. In: *Future Energy:*

Improved, Sustainable and Clean Options for Our Planet (Letcher, T. M., ed.). Elsevier, 2013, 117–143. https://doi.org/10.1016/B978-0-08-099424-6.00006-5
19. Speight, J. G. Origin and properties of oil shale. In: *Shale Oil Production Processes*. Elsevier, 2012, 1–33. https://doi.org/10.1016/b978-0-12-401721-4.00001-1
20. Bai, F., Sun, Y., Liu, Y., Li, Q., Guo, M. Thermal and kinetic characteristics of pyrolysis and combustion of three oil shales. *Energy Convers. Manag.*, 2015, **97**, 374–381. https://doi.org/10.1016/j.enconman.2015.03.007
21. Urov, K., Sumberg, A. Characteristics of oil shales and shale-like rocks of known deposits and outcrops. *Oil Shale*, 1999, **16**(3S), 1–64.
22. Luik, H., Luik, L., Tiikma, L., Vink, N. Parallels between slow pyrolysis of Estonian oil shale and forest biomass residues. *J. Anal. Appl. Pyrolysis*, 2007, **79**(1–2), 205–209. https://doi.org/10.1016/j.jaap.2006.12.003
23. Ristic, N. D., Djokic, M. R., Konist, A., Van Geem, K. M., Marin, G. B. Quantitative compositional analysis of Estonian shale oil using comprehensive two dimensional gas chromatography. *Fuel Process. Technol.*, 2017, **167**, 241–249. https://doi.org/10.1016/j.fuproc.2017.07.008
24. Kiliç, M., Pütün, A. E., Uzun, B. B., Pütün, E. Converting of oil shale and biomass into liquid hydrocarbons via pyrolysis. *Energy Convers. Manag.*, 2014, **78**, 461–467. https://doi.org/10.1016/j.enconman.2013.11.002
25. Nazzal, J. M. The influence of grain size on the products yield and shale oil composition from the pyrolysis of Sultani oil shale. *Energy Convers. Manag.*, 2008, **49**(11), 3278–3286. https://doi.org/10.1016/j.enconman.2008.03.028
26. Jin, Q., Wang, X., Li, S., Mikulčić, H., Bešenić, T., Deng, S., Vujanović, M., Tan, H., Kumfer, B. M. Synergistic effects during co-pyrolysis of biomass and plastic: gas, tar, soot, char products and thermogravimetric study. *J. Energy Inst.*, 2019, **92**(1), 108–117. https://doi.org/10.1016/j.joei.2017.11.001
27. Ganev, E., Ivanov, B., Vaklieva-Bancheva, N., Kirilova, E., Dzhelil, Y. A multi-objective approach toward optimal design of sustainable integrated biodiesel/diesel supply chain based on first- and second-generation feedstock with solid waste use. *Energies*, 2021, **14**(8). https://doi.org/10.3390/en14082261
28. Chen, B., Han, X., Tong, J., Mu, M., Jiang, X., Wang, S., Shen, J., Ye, X. Studies of fast co-pyrolysis of oil shale and wood in a bubbling fluidized bed. *Energy Convers. Manag.*, 2020, **205**, 112356. https://doi.org/10.1016/j.enconman.2019.112356
29. Lyons Cerón, A., Ochieng, R., Sarker, S., Järvik, O., Konist, A. Co-pyrolysis of woody biomass and oil shale – a kinetics and modelling study. *Energies*, 2024, **17**(5), 1055. https://doi.org/10.3390/en17051055
30. Krerkkaiwan, S., Fushimi, C., Tsutsumi, A., Kuchonthara, P. Synergetic effect during co-pyrolysis/gasification of biomass and sub-bituminous coal. *Fuel Process. Technol.*, 2013, **115**, 11–18. https://doi.org/10.1016/j.fuproc.2013.03.044
31. Chen, B., Han, X., Mu, M., Jiang, X. Studies of the co-pyrolysis of oil shale and wheat straw. *Energy Fuels*, 2017, **31**(7), 6941–6950. https://doi.org/10.1021/acs.energyfuels.7b00871

32. Dai, M., Yu, Z., Fang, S., Ma, X. Behaviors, product characteristics and kinetics of catalytic co-pyrolysis spirulina and oil shale. *Energy Convers. Manag.*, 2019, **192**, 1–10. https://doi.org/10.1016/j.enconman.2019.04.032
33. Jiang, H., Deng, S., Chen, J., Zhang, L., Zhang, M., Li, J., Li, S., Li, J. Preliminary study on copyrolysis of spent mushroom substrate as biomass and Huadian oil shale. *Energy Fuels*, 2016, **30**(8), 6342–6349. https://doi.org/10.1021/acs.energyfuels.6b01085
34. Ochieng, R., Lyons Cerón, A., Konist, A., Sarker, S. Experimental and modeling studies of intermediate pyrolysis of wood in a laboratory-scale continuous feed retort reactor. *Bioresour. Technol.*, 2023, **24**, 101650. https://doi.org/10.1016/j.biteb.2023.101650
35. Lyons Cerón, A., Konist, A., Lees, H., Järvik, O. Effect of woody biomass gasification process conditions on the composition of the producer gas. *Sustainability*, 2021, **13**(21), 11763. https://doi.org/10.3390/su132111763
36. Lyons Cerón, A., Konist, A. Co-pyrolysis of woody biomass and oil shale in a batch reactor in CO_2, CO_2-H_2O, and Ar atmospheres. *Energies*, 2023, **16**(7), 3145. https://doi.org/10.3390/en16073145
37. Bridgwater, A. V. Review of fast pyrolysis of biomass and product upgrading. *Biomass Bioenergy*, 2012, **38**, 68–94. https://doi.org/10.1016/j.biombioe.2011.01.048
38. Özbay, G. Catalytic pyrolysis of pine wood sawdust to produce bio-oil: effect of temperature and catalyst additives. *J. Wood Chem. Technol.*, 2015, **35**(4), 302–313. https://doi.org/10.1080/02773813.2014.958240
39. Yorgun, S., Yıldız, D. Slow pyrolysis of paulownia wood: effects of pyrolysis parameters on product yields and bio-oil characterization. *J. Anal. Appl. Pyrolysis*, 2015, **114**, 68–78. https://doi.org/10.1016/j.jaap.2015.05.003
40. Demirbas, A. Effect of temperature on pyrolysis products from biomass. *Energy Sources A: Recovery Util. Environ. Eff.*, 2007, **29**(4), 329–336. https://doi.org/10.1080/009083190965794
41. Grieco, E., Baldi, G. Analysis and modelling of wood pyrolysis. *Chem. Eng. Sci.*, 2011, **66**(4), 650–660. https://doi.org/10.1016/j.ces.2010.11.018
42. Pistis, A., Tugulu, C., Floris, F., Asquer, C., Scano, E. A. Fast pyrolysis of pine wood at pre-industrial scale: yields and products chemical-physical characterisation. In: *Proceedings of 25th European Biomass Conference and Exhibition*, June 12–15, 2017, Stockholm, Sweden. EUBCE, 2017, 1198–1204.
43. Zhou, C., Yang, W. Characterization of the products from spruce and pine sawdust pyrolysis at various temperatures. In: *Proceedings of 21st European Biomass Conference and Exhibition*, June 3–7, 2013, Copenhagen, Denmark. EUBCE, 2013, 968–973.
44. Ningbo, G., Baoling, L., Aimin, L., Juanjuan, L. Continuous pyrolysis of pine sawdust at different pyrolysis temperatures and solid residence times. *J. Anal. Appl. Pyrolysis*, 2015, **114**, 155–162. https://doi.org/10.1016/j.jaap.2015.05.011
45. Demirbas, M. F. Characterization of bio-oils from spruce wood (*Picea orientalis* L.) via pyrolysis. *Energy Sources A: Recovery Util. Environ. Eff.*, 2010, **32**(10),

909–916. https://doi.org/10.1080/15567030903059970
46. Fagernäs, L., Kuoppala, E., Tiilikkala, K., Oasmaa, A. Chemical composition of birch wood slow pyrolysis products. *Energy Fuels*, 2012, **26**(2), 1275–1283. https://doi.org/10.1021/ef2018836
47. Yanik, J., Seçim, P., Karakaya, S., Tiikma, L., Luik, H., Krasulina, J., Raik, P., Palu, V. Low-temperature pyrolysis and co-pyrolysis of Göynük oil shale and terebinth berries (Turkey) in an autoclave. *Oil Shale*, 2011, **28**(4), 469–486. https://doi.org/10.3176/oil.2011.4.02
48. Bozoglu, C., Karayildirim, T., Yanik, J. Utilization of products obtained from copyrolysis of oil shale and plastic. *Oil Shale*, 2009, **26**(4), 475–490. https://doi.org/10.3176/oil.2009.4.04
49. Johannes, I., Tiikma, L., Luik, H. Synergy in co-pyrolysis of oil shale and pine sawdust in autoclaves. *J. Anal. Appl. Pyrolysis*, 2013, **104**, 341–352. https://doi.org/10.1016/j.jaap.2013.06.015
50. Li, S., Chen, X., Liu, A., Wang, L., Yu, G. Co-pyrolysis characteristic of biomass and bituminous coal. *Bioresour. Technol.*, 2015, **179**, 414–420. https://doi.org/10.1016/j.biortech.2014.12.025
51. Bai, J., Chen, X., Shao, J., Jia, C., Wang, Q. Study of breakage of main covalent bonds during co-pyrolysis of oil shale and alkaline lignin by TG-FTIR integrated analysis. *J. Energy Inst.*, 2019, **92**(3), 512–522. https://doi.org/10.1016/j.joei.2018.04.007
52. Hu, Z., Ma, X., Li, L. The synergistic effect of co-pyrolysis of oil shale and microalgae to produce syngas. *J. Energy Inst.*, 2016, **89**(3), 447–455. https://doi.org/10.1016/j.joei.2015.02.009
53. Bieniek, A., Jerzak, W., Magdziarz, A. Experimental studies of intermediate pyrolysis of woody and agricultural biomass in a fixed bed reactor. *E3S Web Conf.*, 2021, **323**, 1–6. https://doi.org/10.1051/e3sconf/202132300003
54. Yang, Y., Brammer, J. G., Mahmood, A. S. N., Hornung, A. Intermediate pyrolysis of biomass energy pellets for producing sustainable liquid, gaseous and solid fuels. *Bioresour. Technol.*, 2014, **169**, 794–799. https://doi.org/10.1016/J.BIORTECH.2014.07.044
55. Maaten, B., Järvik, O., Pihl, O., Konist, A., Siirde, A. Oil shale pyrolysis products and the fate of sulfur. *Oil Shale*, 2020, **37**(1), 51–69. https://doi.org/10.3176/oil.2020.1.03
56. Wiedemeier, D. B., Abiven, S., Hockaday, W. C., Keiluweit, M., Kleber, M., Masiello, C. A., McBeath, A. V., Nico, P. S., Pyle, L. A., Schneider, M. P. W., Smernik, R. J., Wiesenberg, G. L. B., Schmidt, M. W. I. Aromaticity and degree of aromatic condensation of char. *Org. Geochem.*, 2015, **78**, 135–143. https://doi.org/10.1016/j.orggeochem.2014.10.002
57. Okoroigwe, E., Li, Z., Stuecken, T., Saffron, C., Onyegegbu, S. Pyrolysis of *Gmelina arborea* wood for bio-oil/bio-char production: physical and chemical characterisation of products. *J. Appl. Sci*., 2012, **12**(4), 369–374. https://doi.org/10.3923/jas.2012.369.374
58. Lachos-Perez, D., Martins-Vieira, J. C., Missau, J., Anshu, K., Siakpebru, O. K.,

Thengane, S. K., Morais, A. R. C., Tanabe, E. H., Bertuol, D. A. Review on biomass pyrolysis with a focus on bio-oil upgrading techniques. *Analytica*, 2023, **4**(2), 182–205. https://doi.org/10.3390/analytica4020015

59. Tinwala, F., Mohanty, P., Parmar, S., Patel, A., Pant, K. K. Intermediate pyrolysis of agro-industrial biomasses in bench-scale pyrolyser: product yields and its characterization. *Bioresour. Technol.*, 2015, **188**, 258–264. https://doi.org/10.1016/J.BIORTECH.2015.02.006
60. Yadykova, A. Y., Ilyin, S. O. Compatibility and rheology of bio-oil blends with light and heavy crude oils. *Fuel*, 2022, **314**, 122761. https://doi.org/10.1016/J.FUEL.2021.122761
61. Olukcu, N., Yanik, J., Saglam, M., Yuksel, M. Liquefaction of beypazari oil shale by pyrolysis. *J. Anal. Appl. Pyrolysis*, 2002, **64**(1), 29–41. https://doi.org/10.1016/S0165-2370(01)00168-1
62. Mozaffari, S., Järvik, O., Baird, Z. S. Effect of N_2 and CO_2 on shale oil from pyrolysis of Estonian oil shale. *Int. J. Coal Prep. Util.*, 2022, **42**(10), 2908–2922. https://doi.org/10.1080/19392699.2021.1914025
63. Järvik, O., Oja, V. Molecular weight distributions and average molecular weights of pyrolysis oils from oil shales: literature data and measurements by size exclusion chromatography (SEC) and atmospheric solids analysis probe mass spectroscopy (ASAP MS) for oils from four different deposits. *Energy Fuels*, 2017, **31**(1), 328–339. https://doi.org/10.1021/acs.energyfuels.6b02452
64. Jin, F., Liu, P., Chen, L., Hua, D., Yi, X. Study on the thermal stability of the bio-oil components by Py-GC/MS. *Energy Reports*, 2023, **9**(4), 280–288. https://doi.org/10.1016/j.egyr.2023.04.001
65. Zandersons, J., Dobele, G., Jurkjane, V., Tardenaka, A., Spince, B., Rizhikovs, J., Zhurins, A. Pyrolysis and smoke formation of grey alder wood depending on the storage time and the content of extractives. *J. Anal. Appl. Pyrolysis*, 2009, **85**(1–2), 163–170. https://doi.org/10.1016/j.jaap.2008.11.036
66. Zhang, L., Shen, C., Liu, R. GC–MS and FT–IR analysis of the bio-oil with addition of ethyl acetate during storage. *Front. Energy Res.*, 2014, **2**, 75175. https://doi.org/10.3389/fenrg.2014.00003
67. dos Santos, A. L., Lucas, A. N. L., da Mota, I. D. P., Schneider, J. K., Polidoro, A. S., Pinho, A. R., Mendes, F. L., Caramão, E. B. Quantitative GC–MS analysis of sawdust bio-oil. *J. Braz. Chem. Soc.*, 2023, **34**(11), 1581–1591. https://doi.org/10.21577/0103-5053.20230060
68. Patra, S. C., Vijay, M., Panda, A. K. Production and characterisation of bio-oil from Gold Mohar (*Delonix regia*) seed through pyrolysis process. *Int. J. Ambient Energy*, 2017, **38**(8), 788–793. https://doi.org/10.1080/01430750.2016.1222958
69. Sugumaran, V., Prakash, S., Ramu, E., Arora, A. K., Bansal, V., Kagdiyal, V., Saxena, D. Detailed characterization of bio-oil from pyrolysis of non-edible seed-cakes by Fourier Transform Infrared Spectroscopy (FTIR) and gas chromatography mass spectrometry (GC–MS) techniques. *J. Chromatogr. B*, 2017, **1058**, 47–56. https://doi.org/10.1016/J.JCHROMB.2017.05.014